mathematics

Article

Adaptive Event-Triggered Neural Network Fast Finite-Time Control for Uncertain Robotic Systems

Jianhui Wang [1], Yongping Du [1], Yuanqing Zhang [1], Yixiang Gu [1] and Kairui Chen [1,2,*]

1 School of Mechanical and Electrical Engineering, Guangzhou University, Guangzhou 510006, China; jhwang@gzhu.edu.cn (J.W.); 2112107046@e.gzhu.edu.cn (Y.D.); 2007200145@e.gzhu.edu.cn (Y.Z.); 32107300046@e.gzhu.edu.cn (Y.G.)
2 School of Computer & Information, Qiannan Normal University for Nationalities, Duyun 558000, China
* Correspondence: kray@gzhu.edu.cn

Abstract: A fast convergence adaptive neural network event-triggered control strategy is proposed for the trajectory tracking issue of uncertain robotic systems with output constraints. To cope with the constraints on the system output in the actual industrial field while reducing the burden on communication resources, an adaptive event-triggered mechanism is designed by using logarithm-type barrier Lyapunov functions and an event-triggered mechanism. Meanwhile, the combination of neural networks and fast finite-time stability theory can not only approximate the unknown nonlinear function of the system, but also construct the control law and adaptive law with a fractional exponential power to accelerate the system's convergence speed. Furthermore, the tracking errors converge quickly to a bounded and adjustable compact set in finite time. Finally, the effectiveness of the strategy is verified by simulation examples.

Keywords: robotic systems; output constraints; fast finite-time stability; event-triggered mechanism

MSC: 93D40

check for updates

Citation: Wang, J.; Du, Y.; Zhang, Y.; Gu, Y.; Chen, K. Adaptive Event-Triggered Neural Network Fast Finite-Time Control for Uncertain Robotic Systems. *Mathematics* **2023**, *11*, 4841. https://doi.org/10.3390/math11234841

Academic Editor: Dimplekumar N. Chalishajar

Received: 1 November 2023
Revised: 25 November 2023
Accepted: 29 November 2023
Published: 1 December 2023

1. Introduction

In modern industrial systems, the constrained robot control problem has gradually become a hot research field. Constraints can restrict the system output during operation, ensuring the safety specifications and the system control performance, and have been extensively studied by scholars [1–6]. In [1], the tangent-type barrier Lyapunov function (BLF) is introduced to ensure that the output remains in the constrained region. In [2], a logarithm-type BLF and the Moore–Penrose inverse term are employed to prevent contravention of output and state constraints. In [3], an integral-type BLF is employed in a two-DOF helicopter system. In [6], an integral-type BLF is introduced to cope with symmetric output constraints, so that the system output conforms to the specified restrictions. In fact, a constant constraint is a typical situation in time-varying constraints. Moreover, methods to deal with time-varying constraints usually combine the time-varying BLF with fuzzy logic systems (FLSs) [7–9] or neural networks (NNs) [10–12]. In [7], an output feedback control approach for an adaptive fuzzy state observer is designed by employing the time-varying BLF. In [10], the time-varying BLF and NNs are used to ensure that the output is limited to a time-varying interval, and the n-link robotic systems are transformed into a class of MIMO systems, which makes them more versatile in dealing with practical problems.

Lyapunov stability theory is one of the most traditional and widely used methods for analyzing the stability of dynamic systems [13–16]. Only when time tends to infinity can the states of the system converge to an equilibrium point. In [13], a diagonal recurrent neural network (DRNN) is utilized for the adaptive control of nonlinear dynamic systems. Furthermore, update rules are developed using Lyapunov stability criteria to further adjust various parameters of the DRNN. Lastly, tests are conducted on parameter variations and disturbance signals to verify the robustness of the proposed control scheme. In [14], the authors proposed a time-domain locally recursive radial basis function network structure for nonlinear system modeling and adaptive control. The main feature of this study is the introduction of discrete Lyapunov stability in order to ensure the asymptotic stability of the system, and conditions on the learning rate are derived using this method. In the simulation study, the performance of a recurrent Elman neural network, a DRNN, a dynamic radial basis function network and a dynamic feedforward neural network is also compared. In [15], a new higher-order contextual hierarchical recursive pi-sigma neural network (CLRPSNN) is proposed. In order to adjust the weights of the proposed CLRPSNN model, a learning process is developed by combining BP and Lyapunov stability methods. The proposed model has better results compared to a PSNN, a feedforward neural network (FFNN) (containing a single hidden layer) and various popular recurrent neural networks (RNNs). In [16], an adaptive dynamic programming control and identification scheme for nonlinear dynamical systems is designed with the control objective that the output of the controlled object follows the desired trajectory. The gradient descent (GD) and Lyapunov stability (LS) criterion methods are used to derive the weight-updating equations for all the neural networks in the scheme. The global stability of the system is guaranteed by the weight-updating equations obtained by the LS criterion, and the final results show that the LS method is more accurate than the GD method.

In contrast, however, fast-finite time stabilization theory focuses on analyzing the ability of a system to reach a steady state in a finite time. The fast-finite time control method has rapid convergence speeds, high precision and strong robustness to uncertainty. Therefore, in recent years, many scholars have proposed a variety of finite-time stable design mechanisms [17–23]. For instance, in [17], semi-global practical finite-time stability theory is proposed, and a finite-time adaptive control approach to state feedback is proposed in combination with NNs. Nonetheless, when its preliminary state is away from the origin, the convergence speed of this control strategy will be reduced. In order to overcome this problem, in [18], it was found that, according to the fast finite-time stability criterion, the Lyapunov function satisfies $\dot{V}(x) \leq -aV(x) - \beta V^h(x) + \varrho$. Furthermore, in [19], the dynamic surface control technique is utilized, the boundary conditions of the gain function are relaxed and an adaptive fast finite-time output tracking control approach is designed for reducing the computational complexity.

On the other hand, the above research achievements are based on a traditional time-triggered mechanism (TTM). The sampling period is fixed and the communication bandwidth is limited, thus leading to the data signal in the network transmission process being prone to delays, affecting the quality of network communication. Therefore, event-triggered mechanisms (ETMs) have attracted an increasing number of scholars' attention [24–32]. In [24], the recent advances in event-triggered control mechanisms are summarized and discussed. In [25], an adaptive NN control strategy for TTM and ETM is designed, and comparative simulation experiments are conducted to further show that the adaptive NN event-triggered control strategy has stronger robustness. In [26], considering uncertain nonlinear systems, an event-triggered prescribed settling time consensus adaptive compensation control method is proposed by using the relative threshold ETM. Furthermore, in [28], by relaxing the permissible error scope of event triggering and integrating the state model error into the construction of compound conditions and the adaptive law of NNs, the amount of trigger moments is decreased significantly. In [33], in order to avoid the continuous sampling of the controller, a method without considering the Zeno current is proposed. The event trigger mechanism of an image is used, and the unmeasurable state variables are reconstructed by multi-filters, which transforms the unknown time-varying parameters and sensor sensitivity into an estimation problem with unknown parameters. Thus, the event-triggered control of robotic systems has certain research significance and is challenging.

Based on the above, considering an uncertain robot with output constraints, an adaptive event-triggered NN fast finite-time control approach is proposed. Under the condition that the system output remains within the predefined constraint interval, all closed-loop system signals are bounded and the tracking errors rapidly converge to a small and adjustable set. The primary innovations can be generalized as follows:

1. Adaptive event-triggered control is designed by using the logarithm-type BLF and the ETM, which effectively reduces the update frequency of the transmitted information between the controller and the actuator while ensuring that the outputs of the robotic systems remain within the predefined constraint interval.
2. Using fast finite-time stability theory, an adaptive NN control approach is proposed. In particular, while compensating for system uncertainties, the system's convergence speed is also accelerated, so that the tracking error quickly converges to a bounded and adjustable compact set within a finite time to improve the system's robustness.

Then the research is divided into 5 sections. Section 2 details the problem exposition and preliminaries. Section 3 introduces the design of event-triggered fast finite-time control and analyzes its stability. Section 4 verifies the effectiveness of the proposed approach through two simulation examples. At last, Section 5 is the conclusion.

2. Problem Description and Preliminaries

2.1. System Exposition

The dynamics of an n-degree of freedom (n-DOF) rigid robotic system [34] can be described as

$$H(w)\ddot{w} + K(w,\dot{w})\dot{w} + D(w) + \mathcal{P}^T(w)Z(t) = \varphi(t) \tag{1}$$

where the position, velocity, acceleration and input torque are $w, \dot{w}, \ddot{w}, \varphi(t) \in \mathcal{R}^n$, respectively. $\mathcal{P}(w)$ is the reversible and unknown Jacobian matrix and $Z(t) \in \mathcal{R}^n$ is the constrained vector force exerted by human and environment. $H(w) \in R^{n\times n}$ represents an unknown inertia matrix. The unknown Coriolis and centripetal torque is denoted as $K(w,\dot{w}) \in \mathcal{R}^{n\times n}$. $D(w) \in \mathcal{R}^n$ is the unknown gravitational force.

Property 1 ([35,36])**.** *The matrix $\dot{H}(w) - 2K(w,\dot{w})$ is skew-symmetric such that $W^T\left(\dot{H}(w) - 2K(w,\dot{w})\right)W = 0$ and $\forall W \in \mathcal{R}^n$, where $H(w)$ is positive definite and symmetric.*

Then, let $x_1 = w$, $x_2 = \dot{w}$. The dynamics of the robotic system (1) are transformed into the following equation

$$\begin{cases} \dot{x}_1 = x_2 \\ \dot{x}_2 = H^{-1}\left(\varphi - \mathcal{P}^T Z - Kx_2 - D\right) \\ y = x_1 \end{cases} \tag{2}$$

where, for convenience, $H, \varphi, \mathcal{P}, K, D$ and Z are abbreviations of $H(x_1)$, $\varphi(t)$, $\mathcal{P}(x_1)$, $K(x_1,x_2)$, $D(x_1)$ and $Z(t)$, respectively. $x_1 = [x_{11}, x_{12}, \ldots, x_{1n}]^T$, $x_2 = [x_{21}, x_{22}, \ldots, x_{2n}]^T \in \mathcal{R}^n$ and y represents the system output. Meanwhile, there exists a constant vector $\bar{k}_{v1} = \left[\bar{k}_{v11}, \bar{k}_{v12}, \ldots, \bar{k}_{v1n}\right]^T \in \mathcal{R}^n$, such that the system output constraint satisfies $|x_1| \le \bar{k}_{v1}$.

Assumption 1 ([37])**.** *The desired signal vector $y_s = [y_{s1}, y_{s2}, \ldots, y_{sn}]^T \in \mathcal{R}^n$ and its first-order derivative $\dot{y}_s = [\dot{y}_{s1}, \dot{y}_{s2}, \ldots, \dot{y}_{sn}]^T \in \mathcal{R}^n$ are both continuous and bounded. There exist positive constant vectors S_0 and S_1 such that $|y_s| \le S_0 \le \bar{k}_{v1}$ and $|\dot{y}_s| \le S_1$.*

Assumption 2 ([38])**.** *Assume that for any $t \in [0,\infty)$, the constrained force $Z(t)$ is uniformly bounded, and there exists $\bar{Z} > 0$, which satisfies $|Z(t)| \le \bar{Z}$.*

Lemma 1 ([19])**.** *Considering a general system $\dot{x} = f(x,w)$, if there exists a continuous function $V(x,t)$, $\gamma_1 > 0$, $\gamma_2 > 0$, $\varrho \in (0,\infty)$ and $h \in (0,1)$ such that*

$$\dot{V}(x,t) \le -\gamma_1 V(x,t) - \gamma_2 V(x,t)^h + \varrho \tag{3}$$

then the trajectory of system $\dot{x} = f(t, w)$ is practically fast finite-time stable. Then, the residual set of the system solution is described as follows

$$\Xi = \left\{ x | V(x,t) \leq \min\left\{ \frac{\varrho}{(1-\omega_0)\gamma_1}, \left(\frac{\varrho}{(1-\omega_0)\gamma_2} \right)^{\frac{1}{h}} \right\} \right\} \tag{4}$$

where $\omega_0 \in (0,1)$. The convergence time T_m is

$$T_m = \max\left\{ t_0 + \frac{1}{\omega_0\gamma_1(1-h)} \ln \frac{\omega_0\gamma_1 V(t_0)^{1-h} + \gamma_2}{\gamma_2}, t_0 + \frac{1}{\gamma_1(1-h)} \ln \frac{\gamma_1 V(t_0)^{1-h} + \omega_0\gamma_2}{\omega_0\gamma_2} \right\} \tag{5}$$

Lemma 2 ([39]). *For $\forall \vartheta_j \in \mathcal{R}$, $j = 1, 2, \ldots, n$ and $a \in [0,1]$, the following inequality holds*

$$\left(\sum_{j=1}^{n} |\vartheta_j| \right)^a \leq \sum_{j=1}^{n} |\vartheta_j|^a \tag{6}$$

Lemma 3 ([40]). *For any δ, $\mu \in \mathcal{R}$, one has*

$$0 \leq |\delta| - \delta \tanh\left(\frac{\delta}{\mu} \right) \leq 0.2785\mu \tag{7}$$

Lemma 4 ([41]). *For any $\kappa_1 > 0$, $\kappa_2 > 0$, $\kappa_3 > 0$, $\psi_1 > 0$, $\psi_2 > 0$ and $\psi_3 > 0$, the following inequality holds*

$$\psi_1^{\kappa_1}\psi_2^{\kappa_2}\psi_3 \leq \kappa_3\psi_1^{\kappa_1+\kappa_2} + \frac{\kappa_2}{\kappa_1+\kappa_2} \times \left[\frac{\kappa_1}{\kappa_3(\kappa_1+\kappa_2)} \right]^{\frac{\kappa_1}{\kappa_2}} \psi_2^{\kappa_1+\kappa_2} \psi_3^{\frac{\kappa_1+\kappa_2}{\kappa_2}} \tag{8}$$

2.2. Radial Basis Function Neural Networks

Radial basis function neural networks (RBFNNs) are widely applied in arbitrary approximation to deal with the environmental uncertainties in nonlinear systems. The general form of RBFNNs can be described as

$$M(Y) = U^T N(Y) + \epsilon(Y) \tag{9}$$

where $Y \in \mathcal{R}^n$ is the input vector; $U = [U_1, U_2, \ldots, U_n]^T$ represents the ideal weight vector; and $N(Y) = [N_1(Y), N_2(Y), \ldots, N_n(Y)]^T$ is the basis function vector, where n is the number of nodes. $\epsilon(Y)$ denotes approximation error such that $|\epsilon(Y)| \leq \bar{\epsilon}$. The Gaussian function is usually chosen as follows

$$N_i(Y) = -\exp\left(\frac{(Y-m_i)^T(Y-m_i)}{u_i^2} \right), i = 1, 2, \ldots, n \tag{10}$$

where u_i and m_i, respectively, represent the width and center of the Gaussian function.

3. Adaptive Event-Triggered Fast Finite-Time Control Design

3.1. Control Design

Firstly, the following error system has been defined as

$$\begin{cases} \xi_1 = x_1 - y_s \\ \xi_2 = x_2 - \alpha_1 \end{cases} \tag{11}$$

where $\xi_1 = [\xi_{11}, \xi_{12}, \ldots, \xi_{1n}]^T$ and $\xi_2 = [\xi_{21}, \xi_{22}, \ldots, \xi_{2n}]^T$; $y_s = [y_{s1}, y_{s2}, \ldots, y_{sn}]$ denotes the desired signal vector; and $\alpha_1 = [\alpha_{11}, \alpha_{12}, \ldots, \alpha_{1n}]^T$ represents the virtual control law.

From (11), the derivative of ξ_1 can be written as

$$\dot{\xi}_1 = \xi_2 + \alpha_1 - \dot{y}_s \tag{12}$$

$$\dot{\xi}_{1i} = \xi_{2i} + \alpha_{1i} - \dot{y}_{si} \tag{13}$$

where $i = 1, 2, \ldots, n$. Choosing the first BLF as

$$V_1 = \sum_{i=1}^{n} \frac{1}{2} \log \frac{k_{1i}^2}{k_{1i}^2 - \xi_{1i}^2} \tag{14}$$

where $k_1 = \bar{k}_{v1} - S_0 = [k_{11}, k_{12}, \ldots, k_{1n}]^T$, then $\dot{V}_1$ can be expressed as

$$\dot{V}_1 = \sum_{i=1}^{n} \frac{\xi_{1i}(\xi_{2i} + \alpha_{1i} - \dot{y}_{si})}{k_{1i}^2 - \xi_{1i}^2} \tag{15}$$

α_{1i} is designed as follows

$$\alpha_{1i} = -z_{1i}\xi_{1i} - \frac{s_{1i}\xi_{1i}^{2h-1}}{(k_{1i}^2 - \xi_{1i}^2)^{h-1}} + \dot{y}_{si} \tag{16}$$

where z_{1i} and s_{1i} are positive constants and $h \in (\frac{1}{2}, 1)$.

By substituting (16) into (15), one has

$$\dot{V}_1 \leq -\sum_{i=1}^{n} \frac{z_{1i}\xi_{1i}^2}{k_{1i}^2 - \xi_{1i}^2} - \sum_{i=1}^{n} \frac{s_{1i}\xi_{1i}^{2h}}{(k_{1i}^2 - \xi_{1i}^2)^h} + \sum_{i=1}^{n} \frac{\xi_{1i}\xi_{2i}}{k_{1i}^2 - \xi_{1i}^2} \tag{17}$$

From (2) and (11), the derivative of ξ_2 can be written as

$$\dot{\xi}_2 = H^{-1}\Big(\varphi - \mathcal{P}^T Z - Kx_2 - D\Big) - \dot{\alpha}_1 \tag{18}$$

Considering the second BLF as

$$V_2 = V_1 + \frac{1}{2}\xi_2^T H \xi_2 \tag{19}$$

and taking the derivative of V_2 and combining it with (17) and (18), it can be obtained that

$$\begin{aligned} \dot{V}_2 \leq & -\sum_{i=1}^{n} \frac{z_{1i}\xi_{1i}^2}{k_{1i}^2 - \xi_{1i}^2} - \sum_{i=1}^{n} \frac{s_{1i}\xi_{1i}^{2h}}{(k_{1i}^2 - \xi_{1i}^2)^h} + \sum_{i=1}^{n} \frac{\xi_{1i}\xi_{2i}}{k_{1i}^2 - \xi_{1i}^2} \\ & + \xi_2^T\Big(\varphi - \mathcal{P}^T Z - Kx_2 - D - H\dot{\alpha}_1\Big) + \frac{1}{2}\xi_2^T \dot{H} \xi_2 \end{aligned} \tag{20}$$

Then, according to Property 1 and $\xi_2 = x_2 - \dot{\alpha}_1$, Equation (20) can be further rewritten as

$$\begin{aligned} \dot{V}_2 \leq & -\sum_{i=1}^{n} \frac{z_{1i}\xi_{1i}^2}{k_{1i}^2 - \xi_{1i}^2} - \sum_{i=1}^{n} \frac{s_{1i}\xi_{1i}^{2h}}{(k_{1i}^2 - \xi_{1i}^2)^h} + \sum_{i=1}^{n} \frac{\xi_{1i}\xi_{2i}}{k_{1i}^2 - \xi_{1i}^2} \\ & + \xi_2^T\Big(\varphi - \mathcal{P}^T Z - K\alpha_1 - D - H\dot{\alpha}_1\Big) \end{aligned} \tag{21}$$

Define the unknown continuous function $M = [M_1(E), M_2(E), \ldots, M_n(E)]^T \in \mathcal{R}^n$ as follows

$$M(E) = -\mathcal{P}^T Z - K\alpha_1 - D - H\dot{\alpha}_1 + \sum_{i=1}^{n} \frac{\xi_{1i}}{k_{1i}^2 - \xi_{1i}^2} \tag{22}$$

where $E = \left[x_1^T, x_2^T, y_s^T, \dot{y}_s^T\right]^T \in \mathcal{R}^{4n}$. By utilizing RBFNNs to approximate the unknown continuous function, it can be described as

$$M_i(E) = W_i^T Q_i(E) + \epsilon_i \tag{23}$$

$$\begin{aligned} \xi_{2i} M_i(E) &= \xi_{2i} W_i^T Q_i(E) + \xi_{2i}\epsilon_i \\ &\leq \frac{1}{2r_i^2}\xi_{2i}^2 \zeta_i \|Q_i\|^2 + \frac{r_i^2}{2} + \frac{\xi_{2i}^2}{2} + \frac{\mu_i^2}{2} \end{aligned} \tag{24}$$

where W_i^T denotes the optimal weight vector; $Q_i(E) = [Q_{i1}(E), Q_{i2}(E), \ldots, Q_{ir}(E)]^T$ represents the radial function vector; r is the amount of nodes; ϵ_i is the approximation error; μ_i is a constant such that $\epsilon_i \leq |\mu_i|$; and $\zeta_i \leq \|W_i\|^2$.

With the help of the relative threshold ETM, the actual control input torque φ_i is introduced to save communication resources. The control input $\varpi_i(t)$ of the ETM is considered as

$$\varpi_i(t) = -(1+\lambda_i)\left[\alpha_{2i}\tanh\left(\frac{\alpha_{2i}\xi_{2i}}{\sigma_i}\right) + b_i \tanh\left(\frac{b_i\xi_{2i}}{\sigma_i}\right)\right] \tag{25}$$

The actual control input $\varphi_i(t)$ is described as

$$\begin{cases} \varphi_i(t) = \varpi_i(t_{i,k}), \quad t_{i,k} \leq t < t_{i,k+1} \\ t_{i,k+1} = \inf\{t \in R \| m_i(t) | \geq \lambda_i |\varphi_i(t)| + o_i\} \end{cases} \tag{26}$$

where λ_i, b_i σ_i and o_i are positive design parameters; $m_i(t) = \varphi_i(t) - \varpi_i(t)$ denotes the measurement error; $b_i > o_i/(1-\lambda_i)$; and $k \in Z^+$.

Remark 1. *While the trigger condition $|m_i(t)| \geq \lambda_i|\varphi_i(t)| + o_i$ is true, the control input signal $\varphi_i(t) = \varpi_i(t_{i,k})$ will be updated and its value will be transmitted to the actuator; conversely, when the trigger condition is false, the control signal that maintains the last moment $\varphi_i(t) = \varpi_{i-1}(t_{i-1,k})$ is transmitted to the actuator. Therefore, the ETM reduces the communication burden of the system by reducing the update frequency of the control signal.*

Equation (26) shows that for any $t \in [t_{i,k}, t_{i,k+1})$, $\varpi_i(t) = (1+\eta_{1i}(t)\rho_i)\varphi_i(t) + \eta_{2i}(t)$, where $|\eta_{1i}(t)| \leq 1$ and $|\eta_{2i}(t)| \leq 1$ are time-varying parameters. Thus, it can be further expressed that

$$\varphi_i(t) = \frac{\varpi_i(t) - \eta_{2i}(t)o_i}{1+\eta_{1i}(t)\lambda_i} \tag{27}$$

According to (26) and (27),

$$\begin{aligned} \xi_{2i}\varphi_i &= -\left(\frac{1+\lambda_i}{1+\lambda_i\eta_{2i}(t)}\left(\xi_{2i}\alpha_{2i}\tanh\left(\frac{\xi_{2i}\alpha_{2i}}{\sigma_i}\right) + \xi_{2i}b_i\tanh\left(\frac{\xi_{2i}b_i}{\sigma_i}\right)\right) + \frac{o_i\eta_{1i}(t)}{1+\lambda_i\eta_{2i}(t)}\right) \\ &\leq |\xi_{2i}\alpha_{2i}| - \xi_{2i}\alpha_{2i}\tanh\left(\frac{\xi_{2i}\alpha_{2i}}{\sigma_i}\right) - |\xi_{2i}\alpha_{2i}| + |\xi_{2i}b_i| - \xi_{2i}b_i\tanh\left(\frac{\xi_{2i}b_i}{\sigma_i}\right) \\ &\leq \xi_{2i}\alpha_{2i} + 0.557\sigma_i \end{aligned} \tag{28}$$

Substituting (23)–(28) into (21), one has

$$\begin{aligned} \dot{V}_2 \leq &-\sum_{i=1}^n \frac{z_{1i}\xi_{1i}^2}{k_{1i}^2 - \xi_{1i}^2} - \sum_{i=1}^n \frac{s_{1i}\xi_{1i}^{2h}}{(k_{1i}^2 - \xi_{1i}^2)^h} + \sum_{i=1}^n \xi_{2i}(\alpha_i + \frac{1}{2r_i^2}\xi_{2i}\zeta_i\|Q_i\|^2 + \frac{\xi_{2i}}{2}) \\ &+ \sum_{i=1}^n \frac{r_i^2}{2} + \sum_{i=1}^n \frac{\mu_i^2}{2} + \sum_{i=1}^n 0.557\sigma_i \end{aligned} \tag{29}$$

The controller law α_{2i} is designed as follows

$$\alpha_{2i} = -c_i\xi_{2i} - b_i\xi_{2i}^{2h-1} - \frac{1}{2r_i^2}\xi_{2i}\hat{\zeta}_i\|Q_i\|^2 - \frac{\xi_{2i}}{2} \tag{30}$$

The third BLF is chosen as

$$V_3 = V_2 + \sum_{i=1}^{n}\frac{1}{2a_i}\tilde{\zeta}_i^2 \tag{31}$$

where $\tilde{\zeta}_i = \zeta_i - \hat{\zeta}_i$. Taking the derivative of V_3 and combining it with (30) and (31), one obtains

$$\begin{aligned}\dot{V}_3 \leq &-\sum_{i=1}^{n}\frac{z_{1i}\xi_{1i}^2}{k_{1i}^2 - \xi_{1i}^2} - \sum_{i=1}^{n}\frac{s_{1i}\xi_{1i}^{2h}}{(k_{1i}^2 - \xi_{1i}^2)^h} - \sum_{i=1}^{n}c_i\xi_{2i}^2 - \sum_{i=1}^{n}b_i\xi_{2i}^{2h} \\ &+ \sum_{i=1}^{n}\frac{1}{a_i}\tilde{\zeta}_i(\frac{1}{2r_i^2}a_i\xi_{2i}^2\|Q_i\|^2 - \dot{\hat{\zeta}}_i) + \sum_{i=1}^{n}(0.557\sigma_i + \frac{r_i^2}{2} + \frac{\mu_i^2}{2})\end{aligned} \tag{32}$$

$\dot{\hat{\zeta}}_i$ is the adaptive law, designed as follows

$$\dot{\hat{\zeta}}_i = \frac{1}{2r_i^2}a_i\xi_{2i}^2\|Q_i\|^2 - \rho_i\hat{\zeta}_i \tag{33}$$

Substituting (33) into (32), one has

$$\begin{aligned}\dot{V}_3 \leq &-\sum_{i=1}^{n}\frac{z_{1i}\xi_{1i}^2}{k_{1i}^2 - \xi_{1i}^2} - \sum_{i=1}^{n}\frac{s_{1i}\xi_{1i}^{2h}}{(k_{1i}^2 - \xi_{1i}^2)^h} - \sum_{i=1}^{n}c_i\xi_{2i}^2 - \sum_{i=1}^{n}b_i\xi_{2i}^{2h} \\ &+ \sum_{i=1}^{n}\frac{1}{a_i}\rho_i\tilde{\zeta}_i\hat{\zeta}_i + \sum_{i=1}^{n}(0.557\sigma_i + \frac{r_i^2}{2} + \frac{\mu_i^2}{2})\end{aligned} \tag{34}$$

By utilizing Young's inequality, one has

$$\sum_{i=1}^{n}\frac{1}{a_i}\rho_i\tilde{\zeta}_i\hat{\zeta}_i \leq -\sum_{i=1}^{n}\frac{1}{2a_i}\rho_i\tilde{\zeta}_i^2 + \sum_{i=1}^{n}\frac{1}{2a_i}\rho_i\zeta_i^2 \tag{35}$$

Substituting (35) into (34), it can be obtained that

$$\begin{aligned}\dot{V}_3 \leq &-\sum_{i=1}^{n}\frac{z_{1i}\xi_{1i}^2}{k_{1i}^2 - \xi_{1i}^2} - \sum_{i=1}^{n}\frac{z_{2i}\xi_{2i}^2}{k_{2i}^2 - \xi_{2i}^2} - \sum_{i=1}^{n}b_i\xi_{2i}^{2h} - \sum_{i=1}^{n}c_i\xi_{2i}^2 \\ &- \left(\sum_{i=1}^{n}\frac{1}{2a_i}\tilde{\zeta}_i^2\right)^h + \left(\sum_{i=1}^{n}\frac{1}{2a_i}\tilde{\zeta}_i^2\right)^h - \sum_{i=1}^{n}\frac{1}{2a_i}\rho_i\tilde{\zeta}_i^2 + \Delta_1\end{aligned} \tag{36}$$

where $\Delta_1 = \sum_{i=1}^{n}\left(\frac{1}{2a_i}\rho_i\zeta_i^2 + \frac{\mu_i^2}{2} + \frac{r_i^2}{2} + 0.557\sigma_i\right)$.

According to Lemma 4, and letting $\kappa_1 = 1 - \kappa_2$, $\kappa_2 = h$, $\kappa_3 = \kappa_1\kappa_2^{\frac{\kappa_2}{\kappa_1}}$, $\psi_1 = 1$, $\psi_2 = \sum_{i=1}^{n}\frac{1}{2a_i}\tilde{\zeta}_i^2$ and $\psi_3 = 1$, it can be obtained that

$$\left(\sum_{i=1}^{n}\frac{1}{2a_i}\tilde{\zeta}_i^2\right)^h \leq \kappa_3 + \sum_{i=1}^{n}\frac{1}{2a_i}\tilde{\zeta}_i^2 \tag{37}$$

Substituting (37) into (36), one has

$$\dot{V}_3 \le \sum_{i=1}^{n} \frac{z_{1i}\xi_{1i}^2}{k_{1i}^2 - \xi_{1i}^2} - \sum_{i=1}^{n} \frac{s_{1i}\xi_{1i}^{2h}}{(k_{1i}^2 - \xi_{1i}^2)^h} - \sum_{i=1}^{n} c_i \xi_{2i}^2 - \sum_{i=1}^{n} b_i \xi_{2i}^{2h} - \sum_{i=1}^{n} \frac{1}{2a_i}\rho_i \tilde{\zeta}_i^2 + \sum_{i=1}^{n} \frac{1}{2a_i}\tilde{\zeta}_i^2 - \left(\sum_{i=1}^{n} \frac{1}{2a_i}\tilde{\zeta}_i^2\right)^h + \Delta_2 \tag{38}$$

where $\Delta_2 = \Delta_1 + \kappa_3$. Furthermore, using Lemma 2 yields

$$\begin{aligned}\dot{V}_3 \le & -2\min\{z_{1i}\}\sum_{i=1}^{n}\frac{1}{2}\log\frac{k_{1i}^2}{k_{1i}^2 - \xi_{1i}^2} - 2^h \min\{s_{1i}\}\left(\sum_{i=1}^{n}\frac{1}{2}\log\frac{k_{1i}^2}{k_{1i}^2 - \xi_{1i}^2}\right)^h \\ & - \min\left\{\frac{2c_i}{\lambda_{max}(H)}\right\}\left(\frac{1}{2}\xi_2^T H \xi_2\right) - \min\left\{\frac{b_i 2^h}{\lambda_{max}^h(H)}\right\}\left(\frac{1}{2}\xi_2^T H \xi_2\right)^h \\ & - \min\{\rho_i - 1\}\left(\sum_{i=1}^{n}\frac{1}{2a_i}\tilde{\zeta}_i^2\right) - \left(\sum_{i=1}^{n}\frac{1}{2a_i}\tilde{\zeta}_i^2\right)^h + \Delta_2\end{aligned} \tag{39}$$

Finally, it can be obtained that

$$\dot{V}_3 \le -\phi V_3 - \chi V_3^h + \Delta_2 \tag{40}$$

where $\phi = \min\left\{2z_{1i}, \frac{2c_i}{\lambda_{max}(H)}, \rho_i - 1\right\}$ and $\chi = \min\left\{2^h s_{1i}, \frac{b_i 2^h}{\lambda_{max}^h(H)}, 1\right\}$.

Remark 2. *In [42], for any $k > 0$ satisfying $|k| < z$, we can obtain that $\log\frac{k^2}{k^2 - z^2} \le \frac{z^2}{k^2 - z^2}$. Therefore, it can be further inferred that $\left(\log\frac{k^2}{k^2-z^2}\right)^h \le \left(\frac{z^2}{k^2-z^2}\right)^h$ holds when $h \in (0,1)$.*

3.2. Stability Analysis

Theorem 1. *Considering n-DOF robotic systems (1) with output constraints under Assumptions 1 and 2, the virtual control laws (16) and (30), adaptive law (33) and ETMs (25) and (26), it is guaranteed that*

1. *All the closed-loop system signals are bounded, and the tracking errors ξ_{1i} rapidly converge to the bounded and adjustable compact set within a finite time.*
2. *The system output does not exceed the predefined constraint interval, and the Zeno phenomenon does not occur successfully.*

Proof of Theorem 1. According to Lemma 1 and (40), in a finite time, the error signals $E = [\xi_{1i}^T, \xi_{2i}^T, \tilde{\zeta}_1, \tilde{\zeta}_2, \ldots, \tilde{\zeta}_n]^T$ can rapidly converge to the following set

$$\Upsilon = \left\{E | V(E) \le min\left\{\frac{\Delta_2}{(1-\kappa)\phi}, \left(\frac{\Delta_2}{(1-\kappa)\chi}\right)^{\frac{1}{h}}\right\}\right\} \tag{41}$$

where $\kappa \in (0,1)$. Then, the convergence time T is given as

$$T \le max\left\{t_0 + \frac{1}{\kappa\phi(1-h)} ln\frac{\kappa\phi V(t_0)^{1-h} + \chi}{\chi}, t_0 + \frac{1}{\phi(1-h)} ln\frac{\phi V(t_0)^{1-h} + \kappa\chi}{\kappa\chi}\right\} \tag{42}$$

Therefore, it can be obtained from (41) that ξ_{1i}, ξ_{2i} and $\tilde{\zeta}_i$ are bounded, as well as y_m, so x_1 and $\hat{\zeta}_i$ are bounded. Further, the boundedness of α_{1i}, x_2 and α_{2i} can be obtained from (11), (16) and (30). As a result of the boundedness of x_2 and α_{2i}, one has that ϖ_i and τ_i are bounded. Thus, all closed-loop system signals are bounded.

Remark 3. *Based on the above analysis, the tracking errors converge to the bounded and adjustable set in Equation (41), which can be adjusted by adjusting the parameters of h, ψ, ϕ and κ. Furthermore, it can be perceived from Equation (44) that the convergence time T is bounded, and its related design parameters are the same as those of the tracking errors. Therefore, selecting appropriate parameter values can not only improve the convergence accuracy, but also accelerate the system's convergence speed.*

According to (11), $|\xi_1| \leq k_1$ and $|y_m| \leq S_0$, and thus one has $x_1| \leq |\xi_1| + |y_m| \leq k_1 + S_0$. Due to $k_1 = \bar{k}_{v1} - S_0$, it can be further obtained that $|x_i| \leq \bar{k}_{vi}$, so the output of the n-DOF robotic system will remain within the predefined constraint interval.

From any $t \in [t_{i,k}, t_{i,k+1})$ and $m_i(t) = \tau_i(t) - \varpi_i(t)$, one has

$$\frac{d|m_i|}{dt} = sgn(m_i)\dot{m}_i \leq |\dot{\varpi}_i| \tag{43}$$

As can be obtained from (27), $\dot{\varpi}_i$ is continuous and bounded, so there is a positive constant $\bar{\varpi}_i$ which satisfies $|\dot{\varpi}_i| < \bar{\varpi}_i$. At the same time, because $lim_{t_k \to t_{k+1}} m_i(t) = \lambda_i|\tau_i(t)| + o_i$ and $m_i(t_k) = 0$, the lower bound of the event-triggered time interval can be expressed as $t^\star \geq (\lambda_i|\tau_i(t)| + o_i)/\bar{\varpi}_i$. Thus, the Zeno phenomenon does not occur successfully. Finally, the proposed control method and its pseudo-code are shown in Figure 1 and Algorithm 1. □

Algorithm 1: The proposed control method

Choose the following controller parameters:
The parameters of α_{1i}: z_{1i}, k_{1i}, s_{1i}, h;
The parameters of α_{2i} and ζ_i: z_{2i}, b_{2i}, r_i, a_i, ρ_i;
Choose the following controller parameters:
Reference output: y_s;
Initializing: $x_i(0)$, $\hat{\zeta}_i(0)$;
State feedback: $x_i(t)$.
FOR EACH t
1. Update the system states by solving (1);
2. α_{1i} is computed by solving (16);
3. α_{2i} and $\hat{\zeta}_i$ are computed by solving (30) and (33), respectively;
4. The control input $\varpi_i(t)$ is calculated by solving (25);
5. Update the control input $\varphi_i(t)$ according to the following rules:
IF $|m_i(t)| \geq \lambda_i|\varphi_i(t)| + o_i$
$\varphi_i(t) = \varpi_i(t)$;
ELSE
$\varphi_i(t)$ keeps the value of the previous moment;
END
6. $\varphi_i(t)$ is applied to the system (2);
END FOR
System output: y.

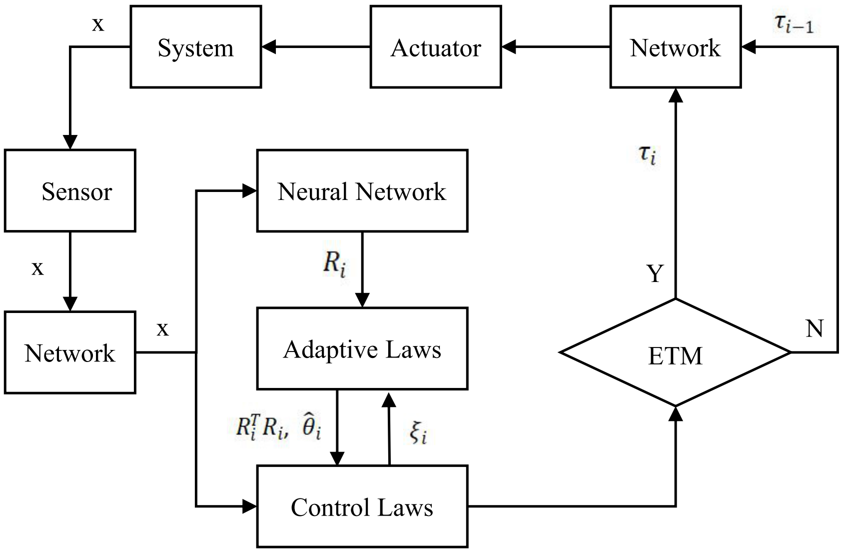

Figure 1. The proposed control method.

4. Simulation

Next, the control strategy designed above will be applied to rigid robotic systems with two DOFs and three DOFs in order to verify its effectiveness through simulations.

4.1. Example A: Two-DOF Rigid Robotic System

A rigid robotic system with two rotary degrees of freedom is considered. We define $x_1 = [w_1, w_2]^T$ and $x_2 = [\dot{w}_1, \dot{w}_2]^T$. $H(x_1)$, $K(x_1, x_2)$, $D(x_1)$ and $\mathcal{P}(x_1)$ are defined as follows

$$H(x_1) = \begin{bmatrix} H_{11} & H_{12} \\ H_{21} & H_{22} \end{bmatrix}$$

$$K(x_1, x_2) = \begin{bmatrix} K_{11} & K_{12} \\ K_{21} & K_{22} \end{bmatrix}$$

$$D(x_1) = \begin{bmatrix} D_{11} \\ D_{21} \end{bmatrix}$$

$$\mathcal{P}(x_1) = \begin{bmatrix} \mathcal{P}_{11} & \mathcal{P}_{12} \\ \mathcal{P}_{21} & \mathcal{P}_{22} \end{bmatrix}$$

where the elements in these matrices are defined in Table 1.

The parameters for the two-DOF rigid robotic system have been chosen as $m_1 = 2.0$ kg, $m_2 = 0.85$ kg, $L_1 = 0.35$ m, $L_2 = 0.31$ m, $I_1 = 61.25 \times 10^{-3}$ kgm^2, $I_2 = 20.42 \times 10^{-3}$ kgm^2 and $g = 9.8$ m/s^2. The vector of constrained force exerted by humans and the environment is considered as $Z(t_s) = [sin(t_s) + 1, 2cos(t_s) + 0.5]^T$. The output constraint interval is defined as $|x_i| \leq 1.5$ rad. The initial position and velocity are considered as $x_{1i}(0) = 0$ and $x_{2i}(0) = 0.1$. The desired signal is selected as $y_s = [sin(2t_s) - 0.3arctan(t) + 0.1, sin(2t_s) - 0.3arctan(t) + 0.1]^T$, where $t_s \in [0, 10]$.

Table 1. Definition of elements in $H(x_1)$, $K(x_1,x_2)$, $D(x_1)$ and $\mathcal{P}(x_1)$.

Elements	Definition	Elements	Definition
H_{11}	$m_1L_{c1}^2+m_2(L_1^2+L_{c2}^2$ $+2L_1L_{c2}cos(w_2))+I_1+I_2$	K_{22}	0
H_{21}	$m_2(L_{c2}^2+L_1L_{c2}cos(w_2))+I_2$	D_{11}	$(m_1L_{c2}+m_2L_1)gcos(w_1)$ $+m_2L_{c2}gcos(w_1+w_2)$
H_{12}	$m_2(L_{c2}^2+L_1L_{c2}cos(w_2))+I_2$	D_{21}	$m_2L_{c2}gcos(w_1+w_2)$
H_{22}	$m_2L_{c2}^2+I_2$	$\mathcal{P}_{11}$	$-L_1sin(w_1)-L_2sin(w_1+w_2)$
K_{11}	$-m_2L_1L_{c2}\dot{w}_2sin(w_2)$	$\mathcal{P}_{21}$	$L_1cos(w_1)+L_2cos(w_1+w_2)$
K_{21}	$m_2L_1L_{c2}\dot{w}_1sin(w_2)$	$\mathcal{P}_{12}$	$-L_2sin(w_1+w_2)$
K_{12}	$-m_2L_1L_{c2}(\dot{w}_1+\dot{w}_2)sin(w_2)$	$\mathcal{P}_{22}$	$L_2cos(w_1+w_2)$

The Gaussian function is selected as

$$Q_i(E)=-\exp\left(\frac{(E-v_i)^T(E-v_i)}{2}\right), i=1,2,\ldots,16 \tag{44}$$

where the center v_i distribution interval of the Gaussian function is $[-1,1]$.

The relevant parameters of the controller are chosen as $h=\frac{4}{5}$, $z_{11}=5$, $z_{12}=7$, $s_{11}=3.5$, $s_{12}=5.3$, $k_{11}=1.5$, $k_{12}=1.5$, $c_1=7$, $c_2=0.7$, $f_1=2$, $f_2=0.1$, $r_1=r_2=1$, $a_1=a_2=1$, $\rho_1=\rho_2=0.1$, $\lambda_1=\lambda_2=\sigma_1=\sigma_2=1$, $o_1=o_2=0.2$, $b_i=o_i/(1-\lambda_i)+0.001$, $\hat{\zeta}_i(0)=0$ and $E=\left[x_1^T,x_2^T,y_s^T,\dot{y}_s^T\right]^T$.

The simulation results from Figures 2 and 3 show that all signals are bounded under output constraints. It is observed from Figure 2a that the joint 1–2 outputs track the given desired trajectory well. The curves of the tracking errors are depicted in Figure 2b, which quickly converge to the compact set within 0.2 s. Figure 2c depicts the curves of the input torque, in which one is the event-triggered control input torque $\varpi_i(t)$, and the other is the control input torque $\tau_i(t)$. Therefore, it shows that the input control signals are bounded. The time interval of event triggering is portrayed in Figure 3a, and the minimum time interval is 0.01 s. Thus, the Zeno phenomenon is eliminated successfully. With the same simulation time and step length, the total triggering time of the traditional TTM is 1000, while the total triggering times of joint 1 and joint 2 are 223 and 317, respectively, shown in Figure 3b,c. It can be perceived that the ETM effectively saves 77.7% and 68.3% of communication resources, respectively.

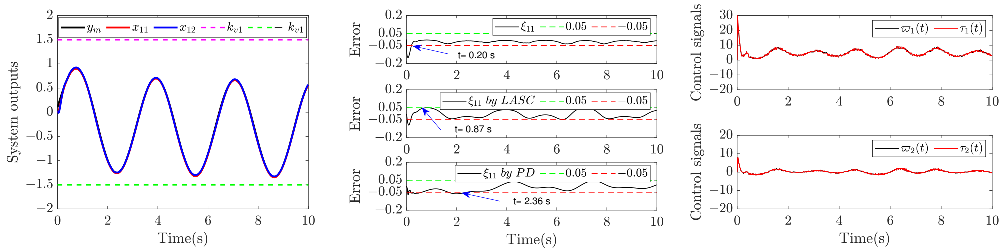

(a) System outputs (b) Tracking errors. (c) Control signals.

Figure 2. The simulation results of Example A.

In addition, it can be seen from Figure 2a,c that the joint 1–2 outputs still track the given desired trajectory well under the premise of considering the constrained force exerted by humans and the environment. The control signal can also realize dynamic compensation, so the proposed control method in this paper has a better robustness.

The above designed control method was compared with Lyapunov asymptotic stability control (LASC) and the PD control method regarding tracking performance; the hyper-parameter selection in these three control methods was consistent. From the simulation results in Figure 2b and Table 2, LASC and the PD control method can also control the tracking error at 0.05 rad. Clearly, the convergence time of the above-designed control scheme is faster, which highlights the superiority of the proposed scheme.

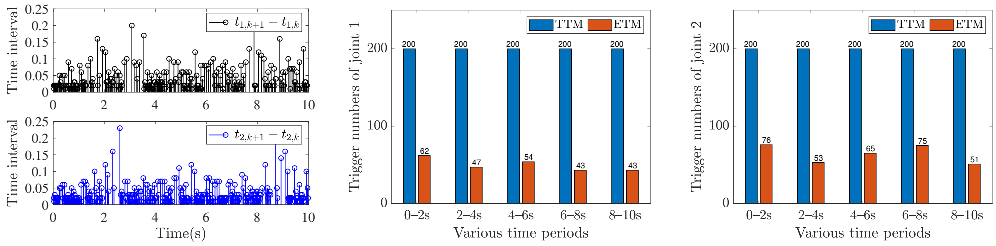

(a) Time intervals. (b) Joint 1's numbers. (c) Joint 2's numbers.

Figure 3. The event-triggered interval and number of Example A.

Table 2. Convergence time of different control methods.

Control Design	Overshoot (rad)	Settling Time (s)
PD	2.36s	0.03
LASC	0.87s	0.04
Proposed control method	0.87s	0.1

4.2. Example B: A Three-DOF Rigid Robotic System

A rigid robotic system with one prismatic degree and two rotary degrees of freedom is considered. We define $x_1 = [w_1, w_2, w_3]^T$ and $x_2 = [\dot{w}_1, \dot{w}_2, \dot{w}_3]^T$. $H(x_1)$, $K(x_1, x_2)$ and $D(x_1)$ are defined as follows

$$H(x_1) = \begin{bmatrix} H_{11} & H_{12} & H_{13} \\ H_{21} & H_{22} & H_{23} \\ H_{31} & H_{32} & H_{33} \end{bmatrix}$$

$$K(x_1, x_2) = \begin{bmatrix} K_{11} & K_{12} & K_{13} \\ K_{21} & K_{22} & K_{23} \\ K_{31} & K_{32} & K_{33} \end{bmatrix}$$

$$D(x_1) = \begin{bmatrix} D_{11} \\ D_{21} \\ D_{31} \end{bmatrix}$$

where the elements in these matrices are defined in Table 3.

Table 3. Definition of elements in $H(x_1)$, $K(x_1, x_2)$ and $D(x_1)$.

Elements	Definition	Elements	Definition
H_{11}	$m_3p_3^2sin^2(w_2) + m_3p_1^2 + m_2p_1^2 + I_1$	K_{13}	$m_3w_3sin^2(w_2)\dot{w}_1$ $-m_3p_1w_3sin(w_2)\dot{w}_2$
H_{12}	$m_3w_3p_1cos(w_2)$		
H_{13}	$m_3p_1sin(w_2)$	K_{21}	$-m_3w_3^2sin(w_2)cos(w_2)\dot{w}_1$
H_{21}	$m_3w_3p_1cos(w_2)$	K_{22}	$m_3w_3\dot{w}_3$
H_{22}	$m_3w_3^2 + I_2$	K_{23}	$m_3p_1cos(w_2)\dot{w}_1 - m_3w_3\dot{w}_2$
H_{23}	0	K_{31}	$-m_3w_3sin^2(w_2)\dot{w}_1$ $+m_3p_1cos(w_2)\dot{w}_2$
H_{31}	$m_3p_1sin(w_2)$		
H_{32}	0	K_{32}	$-m_3w_3\dot{w}_2 + m_3p_1cos(w_2)\dot{w}_2$
H_{33}	m_3	K_{33}	0
K_{11}	$m_3w_3^2sin(w_2)cos(w_2)\dot{w}_2$ $+m_3w_3^2sin^2(w_2)\dot{w}_3$	D_{11}	0
		D_{21}	$-m_3gw_3cos(w_2)$
K_{12}	$m_3w_3^2sin(w_2)cos(w_2)\dot{w}_1$ $-m_3p_1w_3sin(w_2)(\dot{w}_1 + \dot{w}_2)$	D_{31}	$-m_3gsin(w_2)$

The parameters for the three-DOF rigid robotic system were chosen as $m_1 = m_2 = 2$ kg, $m_3 = 1$ kg, $p_1 = 0.3$ m, $p_2 = 0.4$ m, $p_3 = 0.5$ m , $I_1 = \frac{1}{4}m_1 p_1^2$, $I_2 = \frac{1}{4}m_2 p_2^2$, $g = 9.8$ m/s^2, $\mathcal{P}(x_1) = I_{3\times 3}$ and $Z(t_s) = [sin(t_s) + 1, 2cos(t_s) + 0.5, sin(t_s) + 1]^T$. The output constraint interval is defined as $|x_i| \leq 1.5$ rad. The initial position and velocity are considered as $x_{1i}(0) = 0.1$ and $x_{2i}(0) = 0$. The desired trajectory is given as $y_s = [sin(2t_s) - 0.3arctan(t) + 0.1, sin(2t_s) - 0.3arctan(t) + 0.1, sin(2t_s) - 0.3arctan(t) + 0.1]^T$, where $t_s \in [0, 10]$.

The relevant parameters of the controller are designed as $h = \frac{3}{5}$, $z_{11} = 9$, $z_{12} = z_{13} = 13$, $s_{11} = s_{12} = s_{13} = 0.5$, $k_{11} = k_{12} = k_{13} = 1.5$, $c_1 = 8$, $c_2 = c_3 = 11$, $f_1 = f_2 = 2$, $f_3 = 1.5$, $r_1 = r_2 = r_3 = 0.5$, $a_1 = a_2 = a_3 = 0.5$, $\rho_1 = \rho_2 = \rho_3 = 1$, $\lambda_1 = 0.1$, $\sigma_1 = \sigma_2 = \sigma_3 = 1$, $o_1 = 0.7$, $\lambda_2 = \lambda_3 = o_2 = o_3 = 0.2$, $b_i = o_i/(1 - \lambda_i) + 0.001$, $\hat{\zeta}_i(0) = 0$ and $E = \left[x_1^T, x_2^T, y_s^T, \dot{y}_s^T\right]^T$. The basis function is the same as Example A.

According to the simulation results of Figures 4–6, the three-DOF robotic system achieves the expected performance. The system effectively reduces the communication resources while ensuring that the joint outputs maintain within the predefined constraint interval, and the Zeno phenomenon is eliminated successfully. Moreover, the tracking errors quickly converge to a bounded and adjustable compact set within finite time; in particular, the system's convergence speed significantly accelerated.

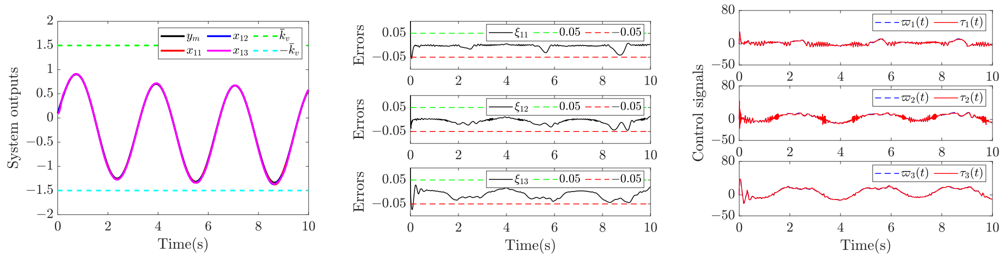

(a) System outputs (b) Tracking errors. (c) Control signals.

Figure 4. The simulation results of Example B.

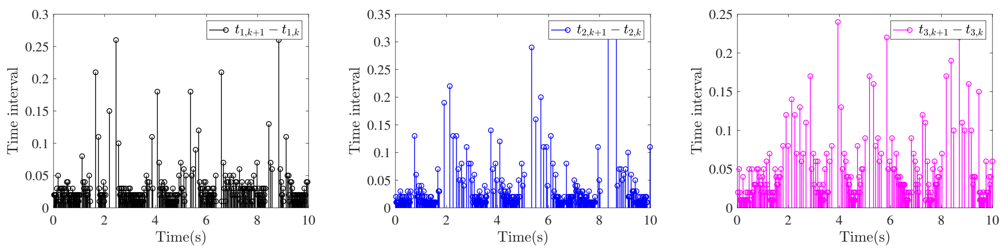

(a) $t_{1,k+1} - t_{1,k}$. (b) $t_{2,k+1} - t_{2,k}$. (c) $t_{3,k+1} - t_{3,k}$.

Figure 5. The event-triggered interval of Example B.

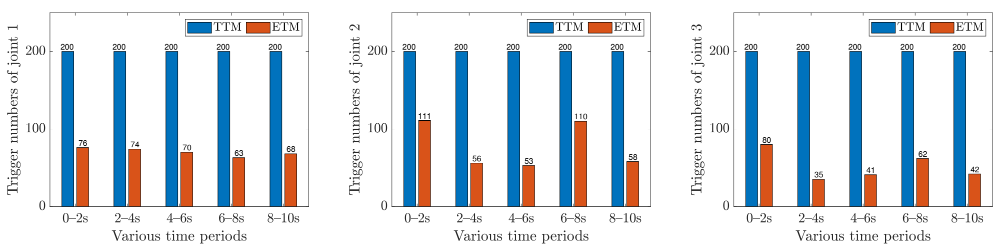

(a) Joint 1's numbers. (b) Joint 2's numbers. (c) Joint 3's numbers.

Figure 6. The event-triggered number of Example B.

5. Conclusions

This paper investigates a category of uncertain robotic systems with output constraints and proposes an adaptive neural network event-triggered control method. By incorporating the logarithm-type BLF and the fast finite-time stability criterion into the backstepping control framework, this approach ensures that the system output is kept within the constraint interval while the tracking errors rapidly converge to a bounded and adjustable compact set in finite time. Simultaneously, the ETM is designed to reduce communication resource consumption by decreasing the control signal update frequency, and Zeno behavior does not successfully occur. Ultimately, the simulation results present evidence of the efficacy of this control method. Meanwhile, artificial neural networks have gradually become a new research hotspot in the field of nonlinear system control, which will be considered in our future related research work.

Author Contributions: Methodology, J.W. and Y.D.; validation, J.W., Y.D. and Y.Z.; formal analysis, Y.G.; data curation, Y.G.; writing—original draft preparation, Y.D. and K.C.; writing—review and editing, J.W. and Y.D.; supervision, Y.Z.; project administration, Y.D. and K.C. All authors have read and agreed to the published version of the manuscript.

Funding: National Natural Science Foundation of China (Grant Number 62103115, 62103153), Guangzhou Yangcheng Scholars Research Project (Grant Number 202235199), Applied basic research talent projects of Guangzhou School (Grant Number RC2023007).

Data Availability Statement: All relevant data are within the paper.

Conflicts of Interest: The authors declare no conflict of interest.

References

1. Yu, X.; He, W.; Li, H.; Sun, J. Adaptive Fuzzy Full-State and Output-Feedback Control for Uncertain Robots with Output Constraint. *IEEE Trans. Syst. Man Cybern. Syst.* **2021**, *51*, 6994–7007. [CrossRef]
2. Zhang, S.; Dong, Y.; Ouyang, Y.; Yin, Z.; Peng, K. Adaptive Neural Control for Robotic Manipulators with Output Constraints and Uncertainties. *IEEE Trans. Neural Netw. Learn. Syst.* **2018**, *29*, 5554–5564. [CrossRef]
3. Ouyang, Y.; Dong, L.; Xue, L.; Sun, C. Adaptive control based on neural networks for an uncertain 2-DOF helicopter system with input deadzone and output constraints. *IEEE/CAA J. Autom. Sin.* **2019**, *6*, 807–815. [CrossRef]
4. Shen, F.; Wang, X.; Yin, X. Adaptive neural output-feedback tracking control for a class of stochastic nonlinear systems with output constraint and unknown control coefficients. *Int. J. Robust Nonlinear Control* **2022**, *32*, 1862–1878. [CrossRef]
5. Sun, Y.; Shi, P.; Lim, C.C. Adaptive consensus control for output-constrained nonlinear multi-agent systems with actuator faults. *J. Frankl. Inst.* **2022**, *359*, 4216–4232. [CrossRef]
6. Xu, Q.; Zong, G.; Chen, Y.; Niu, B.; Shi, K. Command filter-based adaptive neural network controller design for uncertain nonsmooth nonlinear systems with output constraint. *Int. J. Adapt. Control Signal Process.* **2023**, *37*, 474–496. [CrossRef]
7. Liu, Y.J.; Gong, M.; Liu, L.; Tong, S.; Chen, C.L.P. Fuzzy Observer Constraint Based on Adaptive Control for Uncertain Nonlinear MIMO Systems with Time-Varying State Constraints. *IEEE Trans. Cybern.* **2021**, *51*, 1380–1389. [CrossRef]
8. Xu, B.; Li, Y.X.; Ahn, C.K. Small-Gain Approach to Fuzzy Adaptive Control for Interconnected Systems with Unmodeled Dynamics. *IEEE Trans. Fuzzy Syst.* **2022**, *30*, 4702–4716. [CrossRef]
9. Bao, D.; Liang, X.; Ge, S.S.; Hao, Z.; Hou, B. A framework of adaptive fuzzy control and optimization for nonlinear systems with output constraints. *Inf. Sci.* **2022**, *616*, 411–426. [CrossRef]
10. Liu, Y.J.; Lu, S.; Tong, S. Neural Network Controller Design for an Uncertain Robot With Time-Varying Output Constraint. *IEEE Trans. Syst. Man Cybern. Syst.* **2017**, *47*, 2060–2068. [CrossRef]
11. Yang, T.; Sun, N.; Fang, Y.; Xin, X.; Chen, H. New Adaptive Control Methods for *n*-Link Robot Manipulators with Online Gravity Compensation: Design and Experiments. *IEEE Trans. Ind. Electron.* **2022**, *69*, 539–548. [CrossRef]
12. Chen, C.Y.; Tang, Y.; Lu, M.; Yan, H.; Huang, T. Robust adaptive neural control for a class of perturbed nonlinear systems with unmodeled dynamics and output disturbances. *Int. J. Robust Nonlinear Control* **2022**, *32*, 8189–8210. [CrossRef]
13. Kumar, R.; Srivastava, S.; Gupta, J.R.P. Lyapunov stability-based control and identification of nonlinear dynamical systems using adaptive dynamic programming. *Soft Comput.* **2017**, *21*, 4465–4480. [CrossRef]
14. Kumar, R.; Srivastava, S.; Gupta, J.; Mohindru, A. Temporally local recurrent radial basis function network for modeling and adaptive control of nonlinear systems. *ISA Trans.* **2019**, *87*, 88–115. [CrossRef] [PubMed]
15. Kumar, R.; Srivastava, S.; Gupta, J. Diagonal recurrent neural network based adaptive control of nonlinear dynamical systems using lyapunov stability criterion. *ISA Trans.* **2017**, *67*, 407–427. [CrossRef] [PubMed]
16. Kumar, R. A Lyapunov-stability-based context-layered recurrent pi-sigma neural network for the identification of nonlinear systems. *Appl. Soft Comput.* **2022**, *122*, 108836. [CrossRef]

17. Sun, Y.; Chen, B.; Lin, C.; Wang, H. Finite-Time Adaptive Control for a Class of Nonlinear Systems with Nonstrict Feedback Structure. *IEEE Trans. Cybern.* **2018**, *48*, 2774–2782. [CrossRef] [PubMed]
18. Zhang, Y.; Wang, F.; Yan, F. Fast finite time adaptive neural network control for a class of uncertain nonlinear systems subject to unmodeled dynamics. *Inf. Sci.* **2021**, *565*, 306–325. [CrossRef]
19. Wang, H.; Xu, K.; Liu, P.X.; Qiao, J. Adaptive Fuzzy Fast Finite-Time Dynamic Surface Tracking Control for Nonlinear Systems. *IEEE Trans. Circuits Syst. Regul. Pap.* **2021**, *68*, 4337–4348. [CrossRef]
20. Wang, F.; You, Z.; Liu, Z.; Chen, C.L.P. A Fast Finite-Time Neural Network Control of Stochastic Nonlinear Systems. *IEEE Trans. Neural Netw. Learn. Syst.* **2023**, *34*, 7443–7452. [CrossRef]
21. Wang, L.; Liu, P.X.; Wang, H. Fast Finite-Time Control for Nonaffine Stochastic Nonlinear Systems Against Multiple Actuator Constraints via Output Feedback. *IEEE Trans. Cybern.* **2023**, *53*, 3253–3262. [CrossRef]
22. Meng, B.; Liu, W.; Qi, X. Disturbance and state observer-based adaptive finite-time control for quantized nonlinear systems with unknown control directions. *J. Frankl. Inst.* **2022**, *359*, 2906–2931. [CrossRef]
23. Sun, Z.Y.; Shao, Y.; Chen, C.C. Fast finite-time stability and its application in adaptive control of high-order nonlinear system. *Automatica* **2019**, *106*, 339–348. [CrossRef]
24. Peng, C.; Li, F. A survey on recent advances in event-triggered communication and control. *Inf. Sci.* **2018**, *457–458*, 113–125. [CrossRef]
25. Zhang, J.; Niu, B.; Wang, D.; Wang, H.; Zhao, P.; Zong, G. Time-/Event-Triggered Adaptive Neural Asymptotic Tracking Control for Nonlinear Systems with Full-State Constraints and Application to a Single-Link Robot. *IEEE Trans. Neural Netw. Learn. Syst.* **2022**, *33*, 6690–6700. [CrossRef]
26. Wang, J.; Gong, Q.; Huang, K.; Liu, Z.; Chen, C.L.P.; Liu, J. Event-Triggered Prescribed Settling Time Consensus Compensation Control for a Class of Uncertain Nonlinear Systems with Actuator Failures. *IEEE Trans. Neural Netw. Learn. Syst.* **2023**, *34*, 5590–5600. [CrossRef]
27. Wang, J.; Wang, C.; Liu, Z.; Chen, C.L.P.; Zhang, C. Practical Fixed-Time Adaptive ERBFNNs Event-Triggered Control for Uncertain Nonlinear Systems with Dead-Zone Constraint. *IEEE Trans. Syst. Man Cybern. Syst.* **2023**. [CrossRef]
28. Liu, X.; Xu, B.; Shou, Y.; Fan, Q.Y.; Chen, Y. Event-Triggered Adaptive Control of Uncertain Nonlinear Systems with Composite Condition. *IEEE Trans. Neural Netw. Learn. Syst.* **2022**, *33*, 6030–6037. [CrossRef]
29. Wu, J.; He, F.; He, X.; Li, J. Dynamic Event-Triggered Fuzzy Adaptive Control for Non-strict-Feedback Stochastic Nonlinear Systems with Injection and Deception Attacks. *Int. J. Fuzzy Syst.* **2023**, *25*, 1144–1155. [CrossRef]
30. Yang, H.; Ye, D. Adaptive fixed-time bipartite tracking consensus control for unknown nonlinear multi-agent systems: An information classification mechanism. *Inf. Sci.* **2018**, *459*, 238–254. [CrossRef]
31. Wang, J.; Liu, J.; Li, Y.; Chen, C.L.P.; Liu, Z.; Li, F. Prescribed Time Fuzzy Adaptive Consensus Control for Multiagent Systems with Dead-Zone Input and Sensor Faults. *IEEE Trans. Autom. Sci. Eng.* **2023**. [CrossRef]
32. Diao, S.; Sun, W.; Su, S.F.; Xia, J. Adaptive Fuzzy Event-Triggered Control for Single-Link Flexible-Joint Robots with Actuator Failures. *IEEE Trans. Cybern.* **2022**, *52*, 7231–7241. [CrossRef]
33. Meng, R.; Hua, C.; Li, K.; Ning, P. A Multifilters Approach to Adaptive Event-Triggered Control of Uncertain Nonlinear Systems With Global Output Constraint. *IEEE Trans. Cybern.* **2022**. [CrossRef] [PubMed]
34. He, W.; Chen, Y.; Yin, Z. Adaptive Neural Network Control of an Uncertain Robot with Full-State Constraints. *IEEE Trans. Cybern.* **2016**, *46*, 620–629. [CrossRef] [PubMed]
35. Pan, Y.; Du, P.; Xue, H.; Lam, H.K. Singularity-Free Fixed-Time Fuzzy Control for Robotic Systems with User-Defined Performance. *IEEE Trans. Fuzzy Syst.* **2021**, *29*, 2388–2398. [CrossRef]
36. Zhu, C.; Yang, C.; Jiang, Y.; Zhang, H. Fixed-Time Fuzzy Control of Uncertain Robots with Guaranteed Transient Performance. *IEEE Trans. Fuzzy Syst.* **2023**, *31*, 1041–1051. [CrossRef]
37. Rahimi Nohooji, H.; Howard, I.; Cui, L. Neural network adaptive control design for robot manipulators under velocity constraints. *J. Frankl. Inst.* **2018**, *355*, 693–713. [CrossRef]
38. Wu, Y.; Huang, R.; Li, X.; Liu, S. Adaptive neural network control of uncertain robotic manipulators with external disturbance and time-varying output constraints. *Neurocomputing* **2019**, *323*, 108–116. [CrossRef]
39. Li, C.; Zhao, L.; Xu, Z. Finite-Time Adaptive Event-Triggered Control for Robot Manipulators with Output Constraints. *IEEE Trans. Circuits Syst. II Express Briefs* **2022**, *69*, 3824–3828. [CrossRef]
40. Zhao, Y.; Yu, H.; Xia, X. Event-triggered adaptive control of multi-agent systems with saturated input and partial state constraints. *J. Frankl. Inst.* **2022**, *359*, 3333–3365. [CrossRef]
41. Wang, H.; Xu, K.; Qiu, J. Event-Triggered Adaptive Fuzzy Fixed-Time Tracking Control for a Class of Nonstrict-Feedback Nonlinear Systems. *IEEE Trans. Circuits Syst. Regul. Pap.* **2021**, *68*, 3058–3068. [CrossRef]
42. He, W.; David, A.O.; Yin, Z.; Sun, C. Neural Network Control of a Robotic Manipulator with Input Deadzone and Output Constraint. *IEEE Trans. Syst. Man Cybern. Syst.* **2016**, *46*, 759–770. [CrossRef]